Buck-Boost Converter for Sensorless Power Optimization of Piezoelectric Energy Harvester

Elie Lefeuvre, David Audigier, Claude Richard, and Daniel Guyomar

***Abstract*—This paper presents a comprehensive model for miniature vibration-powered piezoelectric generators and analyses modes of operation and control of a buck-boost converter for the purpose of tracking the generators optimal working points. The model describes the generator's power dependence with the mechanical acceleration and frequency, and helps in the definition of the load behaviour for power optimization. Electrical behaviour of the input of buck-boost converter in discontinuous current mode turns out to be in perfect agreement with the considered optimization criteria with a very simple, sensorless control. Experimental results show that the converter controlled by a very low consumption circuit effectively maximizes the power flow into a 4.8 V rechargeable battery connected to the converter output. The converter's efficiency is above 84% for input voltages between 1.6 and 5.5 V, and for output powers between 200 μW and 1.5 mW. The presented circuit and control can be used as well for power optimization of electromagnetic energy harvesting devices.**

***Index Terms*—AC–DC power conversion, dc–dc power conversion, energy conversion, piezoelectric devices, power conditioning, power generation.**

I. Introduction

THE use of piezoelectric materials for converting mechanical energy into electrical energy is not a recent idea. But in practice piezoelectric electrical generators remain limited to very low power domain, usually in the milliwatt range or below. This is mainly due to mechanical properties of piezoelectric ceramics: they accept very large stresses but their strains are very small, making difficult the use of large material quantities. Another point concerns the high mechanical frequencies necessary to effectively use these materials: ambient mechanical vibrations usually remain in the range 0.1 Hz to 1 kHz, whereas piezoelectric materials may work up to hundreds of kilohertz.

Nevertheless, recent development of wearable electronics and wireless systems combined with dramatic progresses in the domain of ultra-low power electronics stimulated extensive researches on recycling of ambient energies [1]–[3]. Use of piezoelectric materials has been in particular investigated for converting ambient mechanical shocks and vibrations into electrical energy [4]–[14]. Arms *et al.* [15] have demonstrated a wireless sensing node including a microprocessor, on-board memory, strain sensing gauge, sensor signal conditioning, and 2.4 Ghz IEEE 802.15.4 radio transceiver with extremely low average consumption: the whole system consumes 900 μW for 10 Hz sampling frequency and 90 μW only for 1 Hz sampling frequency. Development of autonomous sensing nodes powered by piezoelectric generators "harvesting" ambient vibrational energy, usually lost or wasted, is thus already possible with current technologies [16], [17].

Size reduction and effective use of active materials require a careful optimization of such piezoelectric power generators. In particular, they exhibit large effectiveness variations as a function of the load electrical properties. In this field, several optimization circuits and control techniques have been proposed over the past few years [18]–[26].

This paper is focused on power optimization of so-called "seismic" miniature piezoelectric energy harvesters, designed for harvesting mechanical energy resulting from local variations of acceleration which exist, for instance, on an aircraft wings or on a car engine. First, the power optimization problem is examined using a simple but comprehensive electromechanical model of the generator. Operation modes of a buck-boost converter used as power optimization interface are analysed, and conditions for sensorless working are defined. Then, practical implementation of a 1.5 mW power optimization circuit with a sensorless control is demonstrated. Robustness of the control, miniaturization of the converter circuit and possible use for optimizing electromagnetic energy harvesters are discussed before the conclusion.

II. Electromechanical Modeling

Piezoelectric generators designed for harvesting vibratory energy are usually based on mechanical resonators, cantilever beams for instance, able to effectively transmit ambient energy to the active materials. These structures exhibit in general narrow bands of operation near a resonance frequency. The simplest model for such devices is a single mode {spring, mass, damper} mechanical resonator coupled with the electrical circuit through electromechanical properties of the generator's piezoelectric element, as depicted on Fig. 1. On this figure, u_1 and u_2 represent respectively the mechanical displacements of the generator base and the dynamic mass in a Galilean referential. The dynamic mass M undergoes the action of its own inertia, a restoring force due to the mechanical structure stiffness K_S, a viscous force due to the damper C_v and a force F_P due to the piezoelectric element. On the mechanical side, the piezoelectric element acts with its own stiffness K_{PE} plus a voltage controlled force, as expressed in (1), where V_p is the piezoelectric voltage. On the electrical side, the piezoelectric

Manuscript received July 8, 2006; revised January 5, 2007. Recommended for publication by Associate Editor C. Canesin.

The authors are with the Laboratoire de Genie Electrique et Ferroelectricite (LGEF), INSA-Lyon, Villeurbanne Cedex 68621, France (e-mail: elie.lefeuvre @insa-lyon.fr; david.audigier@insa-lyon.fr; claude.richard@insa-lyon.fr; daniel.guyomar@insa-lyon.fr).

Digital Object Identifier 10.1109/TPEL.2007.904230

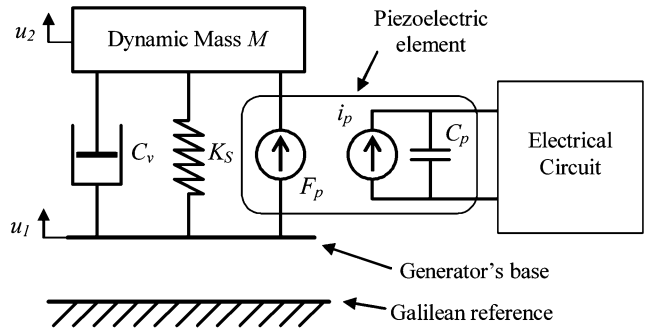

Fig. 1. Electromechanical model of the piezoelectric generator.

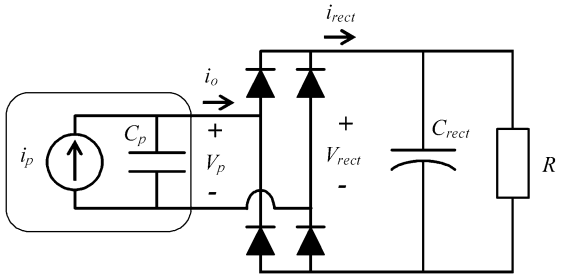

Fig. 2. Electrical circuit with terminal load modelled by a resistor.

internal current source is controlled by the relative mechanical velocity, as expressed in (2). In this equation, α reflects the electromechanical coupling properties of piezoelectric materials. Dynamic equilibrium of the system is defined by (3)

$$F_p = K_{PE}(u_2 - u_1) + \alpha V_p \tag{1}$$

$$i_p = \alpha \frac{d(u_2 - u_1)}{dt} \tag{2}$$

$$M\frac{d^2u_2}{dt^2} + C_v\frac{d(u_2 - u_1)}{dt} + K_S(u_2 - u_1) + F_p = 0. \tag{3}$$

Equations (1)–(3) define the simplest lumped element model for seismic generators usually reported in literature [3],[8]–[10], [26]. In certain cases, the model parameters can be analytically derived from the piezoelectric material properties and from the mechanical setup characteristics. But, generally speaking, parameters values can be predicted using a finite element model [27], and they can also be identified starting from a few measurements on the considered experimental prototype [24]. In spite of its simplicity, this model was shown to be in good agreement with finite element models and with experimental characterization of such generators.

Overall behaviour of the generator can then be derived from these equations and from the electrical behaviour of the electrical circuit. In a first approach, the electrical circuit can be simply composed of a diode bridge, a voltage smoothing capacitor, and a resistor for modelling the power consumed by the terminal load, as shown on Fig. 2. Electrical equations of this circuit [18] and electromechanical (1)–(3) lead to the expression (4) of the average power P produced by the generator in the case of a sinusoidal mechanical displacement u_1 of the generator base at the resonance angular frequency ω_r and

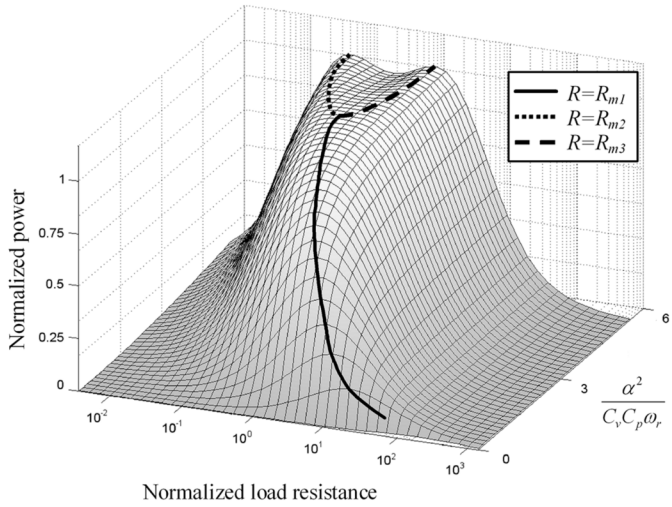

Fig. 3. Normalized power as a function of the normalized load resistance and the electromechanical parameters, at resonance frequency.

with amplitude U_{1M} [24] [see Appendix for detailed derivation at (4)]

$$P = \frac{R\alpha^2}{(RC_p\omega_r + (\pi/2))^2} \frac{M^2\omega_r^4 U_{1M}^2}{(C_v + (2R\alpha^2/(RC_p\omega_r + (\pi/2))^2))^2}. \tag{4}$$

For a given setup with fixed values of parameters M, C_v, $K_S, K_{\mathrm{PE}}, \alpha$ and C_p, (4) shows that the generated average power is proportional to the magnitude of the generator's base acceleration $\omega_r^2 U_{1M}$ squared, but it also depends on the value of the load resistance R. Real positive values R_{m1}, R_{m2} and R_{m3} of the load resistance R which maximize the power are given in (5). There are two possible cases, depending on the electromechanical parameters: the first one with only one matching load resistance $R = R_{m1}$, and the second one with two different matching load resistances $R = R_{m2}$ or $R = R_{m3}$ giving the same maximum power. This is summarized in (6). Power variation as a function of the load resistance and as a function of the electromechanical parameters is represented on Fig. 3.

Most power optimization approaches of piezoelectric electrical generators found in literature do not take into account influence of the load resistance on the magnitude of the piezoelectric current i_p. In this case, only one matching load resistance $R = R_{m1}$ is found. Interest of the model presented herein, taking into account the whole the electromechanical interactions, is to show the possible existence of two other matching load resistances. Moreover, effect of energy harvesting on the mechanical variables can be derived from (1)–(3) and the analysis detailed in the Appendix.

From the power optimization point of view, interpretation of (6) and Fig. 3 is that the generator's power is maximized, whatever the displacement magnitude U_{1M} of the generator's base, on condition that the terminal load behaves like a matching resistor R_m, that is to say the average value of its voltage/current ratio must be equal to the considered value of R_m. Of course, the maximum of power obtained is not constant: its value is related

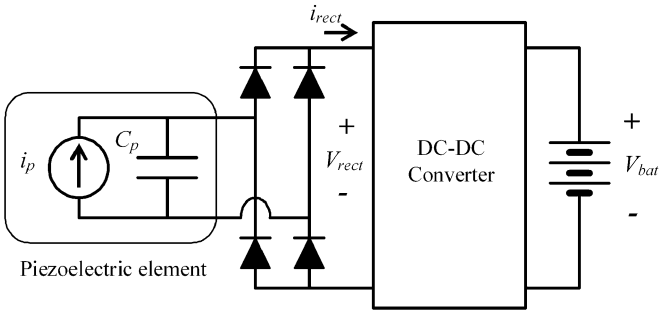

Fig. 4. General circuit for power optimization.

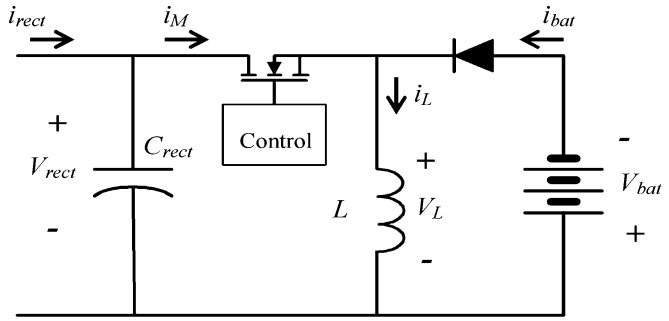

Fig. 5. Buck–Boost converter.

to the displacement magnitude U_{1M} resulting from the ambient vibrations characteristics

$$\begin{cases} R_{m1} = \frac{\pi}{2C_p\omega_r} \\ R_{m2} = \frac{2\alpha^2 - \pi C_v C_p \omega_r - 2\alpha\sqrt{\alpha^2 - \pi C_v C_p \omega_r}}{2C_v(C_p\omega_r)^2} \\ R_{m3} = \frac{2\alpha^2 - \pi C_v C_p \omega_r + 2\alpha\sqrt{\alpha^2 - \pi C_v C_p \omega_r}}{2C_v(C_p\omega_r)^2} \end{cases} \tag{5}$$

$$\begin{cases} \frac{\alpha^2}{C_v C_p \omega_r} \le \pi \Rightarrow R = R_{m1} \text{ and } P_{\max} = \frac{\alpha^2}{2\pi C_p \omega_r} \frac{M^2\omega_r^4 U_{1M}^2}{\left(C_v + \frac{\alpha^2}{\pi C_p \omega_r}\right)^2} \\ \frac{\alpha^2}{C_v C_p \omega_r} > \pi \Rightarrow R = R_{m2} \text{ or } R_{m3} \text{ and } P_{\max} = \frac{M^2\omega_r^4 U_{1M}^2}{8C_v}. \end{cases} \tag{6}$$

III. Power Optimization Circuit

According to the model presented in Section II, the power of a piezoelectric generator strongly depends on the load: the power is maximal for one or two matching load resistances, whose values are determined by the generator electromechanical characteristics and which depend in particular on the vibration frequency of the generator's base. Practically, a seismic piezoelectric generator effectively works in a narrow frequency band around its mechanical resonance, so the matching load resistances can be considered as constant for a given device. In most potential applications, the generator's power may randomly vary as a function of surrounding vibrations. The power need of the load may also vary in more or less important proportions. Continuity of power supply must be ensured by a rechargeable battery or a by supercapacitor, but these energy storage cells don't exhibit the voltage/current properties of a resistor and they can't intrinsically ensure an optimal power generation if directly connected to the rectifier output. Ottman *et al.* [18] have proposed to solve this power optimization problem using a dc–dc converter interleaved between the rectifier and the storage cell, as represented on Fig. 4. They have shown that maximization of the power flowing into the storage cell can be achieved using adaptive controls similar to those used for maximizing the power from solar cells.

In a simpler way, according to the generator's power analysis presented in Section II, the optimal power point can be tracked by controlling the converter so that its input average current is proportional to its input voltage with an average voltage/current ratio equal to the matching load resistance. This optimization technique can be considered as indirect because it is based on the knowledge of the matching load resistance(s) of the considered

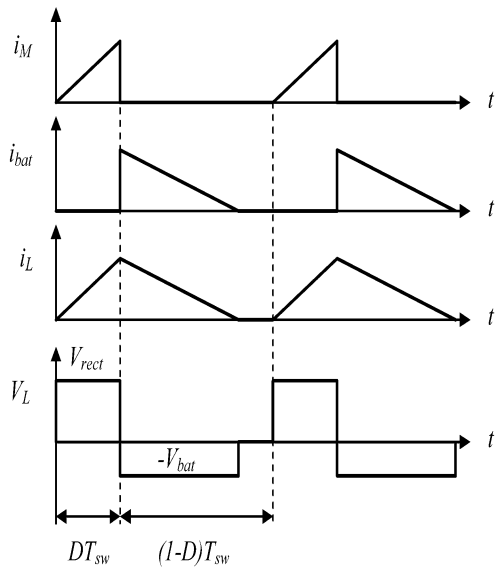

Fig. 6. Currents and voltage waveforms of DCM buck–boost.

electromechanical device. An important point to keep in mind for the design of such an "input average resistance" controlled dc–dc converter is the very weak level of the "harvested" power, typically in the range of hundreds of microwatts. Thus, the control technique must be as simple as possible so that the control circuit consumption can be reduced to a few microwatts. From that point of view, the converter and control described here can be considered as ideal because it neither requires any tracking algorithms nor any sensors. This principle was first proposed by Ottman *et al.* [19], [20] using a buck converter and Kyasap *et al.* [6] using a flyback converter.

The dc–dc converter used here is the buck-boost circuit represented on Fig. 5. The control unit is assumed to turn on and off the MOSFET transistor at the switching frequency $f_{\rm sw}$, with a duty cycle D. The following expressions are established in considering lossless semiconductors. L is considered as a perfect inductor and the voltage ripple of $V_{\rm rect}$ is neglected. Properties of this converter are examined in discontinuous and continuous current modes.

Currents and voltages waveforms of the buck-boost converter in discontinuous current mode (DCM) are represented on Fig. 6. When the transistor is turned on, i_M and i_L are ruled by (7). From this equation is derived the expression (8) of the average currents $\langle i_M \rangle$ and $\langle i_{\rm rect} \rangle$, in which $T_{\rm sw}$ is the switching period

and t_0 an arbitrary time. This equation shows that the average input current of the DCM converter doesn't depend upon the battery voltage and current. Moreover, for fixed values of the duty cycle and the switching frequency, the input average current varies linearly with its input voltage. In other words, the converter input intrinsically exhibits properties similar to those of a resistor, without needing a feedback control. The converter average input resistance $R_{\rm in}$ is expressed in (9)

$$V_{\rm rect} = L\frac{di_L}{dt} = L\frac{di_M}{dt} \tag{7}$$

$$\langle i_M \rangle = \langle i_{\rm rect} \rangle = \frac{1}{T_{\rm sw}} \int_{t_0}^{t_0+T_{\rm sw}} i_M dt = \frac{D^2}{2Lf_{\rm sw}} V_{\rm rect} \tag{8}$$

$$R_{\rm in} = \frac{2Lf_{\rm sw}}{D^2}. \tag{9}$$

In continuous current mode, $V_{\rm rect}$ is linked to $V_{\rm bat}$ and D by

$$V_{\rm rect} = \frac{1-D}{D} V_{\rm bat}. \tag{10}$$

Conservation of input-output energy for the converter leads to the relation (11) between the input voltage and current and the output voltage and current

$$V_{\rm rect} \langle i_{\rm rect} \rangle = V_{\rm bat} \langle i_{\rm bat} \rangle. \tag{11}$$

From (10) and (11), the input voltage on the average input current ratio can be expressed as in (12). This equation shows that the intrinsic property of "constant input average resistance" that was found in DCM doesn't exist anymore in continuous current mode. In this case, a feedback control including sensors would be necessary for tuning the duty cycle so that the average input current varies linearly with the input voltage

$$\frac{V_{\rm rect}}{\langle i_{\rm rect} \rangle} = \left(\frac{1-D}{D} \right)^2 \frac{V_{\rm bat}}{\langle i_{\rm bat} \rangle}. \tag{12}$$

Main advantages of the buck-boost converter for the purpose of power optimization of piezoelectric generators can be summarized as the two following points.

- For fixed values of the duty cycle and the switching frequency, DCM buck-boost converter exhibits a constant input average resistance $R_{\rm in}$ meeting perfectly the optimization criteria of seismic piezoelectric electrical generators.
- This circuit may effectively work whether the converter input voltage $V_{\rm rect}$ is higher or lower than its output voltage $V_{\rm bat}$, enabling optimization of various piezoelectric generators with energy storage cells having various voltages.

Condition for DCM operation is given in (13). This expression allows to practically determining a fixed value of the duty cycle as a function of the voltage of the battery used and as a function of the maximum expected value of the converter input voltage. Then, the inductor and switching frequency can be determined so that the input resistance $R_{\rm in}$ (9) equals the matching load resistance R_m (6) of the piezoelectric device

$$V_{\rm rect} < \frac{1-D}{D} V_{\rm bat}. \tag{13}$$

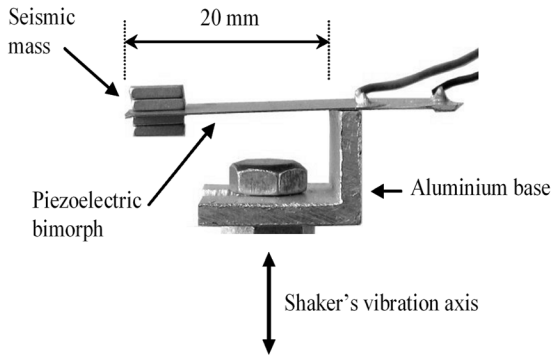

Fig. 7. Piezoelectric generator.

IV. Experimental Results

The generator is a simple cantilever structure, represented on Fig. 7, made up of a $20 \times 14 \times 0.16$ mm^3 piezoelectric bimorph (Murata VSB50EWH0301B, Japan) with 0.76 g seismic mass bonded on the free end. The opposite end of the bimorph is bonded on an aluminium rigid base. The aluminium base of the generator is screwed on an electromagnetic shaker which simulates ambient vibrations. Although the actual generator structure (Fig. 7) and the {spring, mass, damper} model given on Fig. 1 look very different, the behaviour of such a cantilever structure can be faithfully described by the proposed single-dimension mechanical oscillator around a resonance frequency. The considered resonance frequency corresponds here to the first bending mode of the cantilever beam. Seeing that the piezoelectric bimorph mass is negligible compared to the seismic mass attached to the bimorph free end, the dynamic mass M of the model can be considered as equal to the seismic mass. The first bending mode shape and the static flexural shape are practically identical, so the overall stiffness (i.e., the sum K_{PE} plus K_S) is practically equal to the bimorph static flexural stiffness. Overall mechanical losses are modelled by the viscous damping factor C_V. The piezoelectric response, characterized by the α parameter, is here mainly ruled by the lateral electromechanical properties of the active material. The capacitor C_P is the blocking capacitor of the piezoelectric bimorph.

First, the generator has been characterized using the electrical circuit represented on Fig. 2, composed of four BAT86 Schottky diodes, a 10-μF capacitor and a variable resistor. Acceleration of the generator's base was derived from its displacement, monitored by an inductive sensor. According to the results presented on Fig. 8, the generator's power is maximal for load resistances in the 10 kΩ to 18 kΩ range. To make a link with the model presented in Section II, ones can consider that for the considered setup there is only one matching load resistance of approximately 12 kΩ. Power dependence upon the mechanical vibration frequency represented on Fig. 9 shows that the generator operates effectively in a narrow band of approximately 5 Hz around the 66 Hz resonance frequency, which corresponds to the first mechanical bending mode. With the matching load resistance, the rectified voltage $V_{\rm rect}$ is in the 1.1 to 5.5 V range for mechanical RMS accelerations between 0.27 and 2.0 g, as shown on Fig. 10.

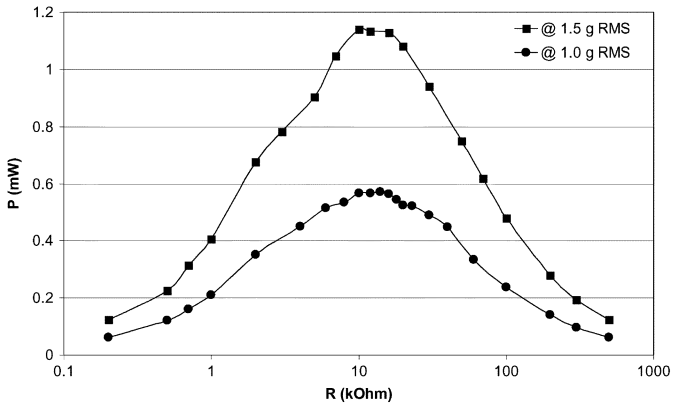

Fig. 8. Load powers versus load resistance at resonance frequency for 1.0 and 1.5 g RMS accelerations.

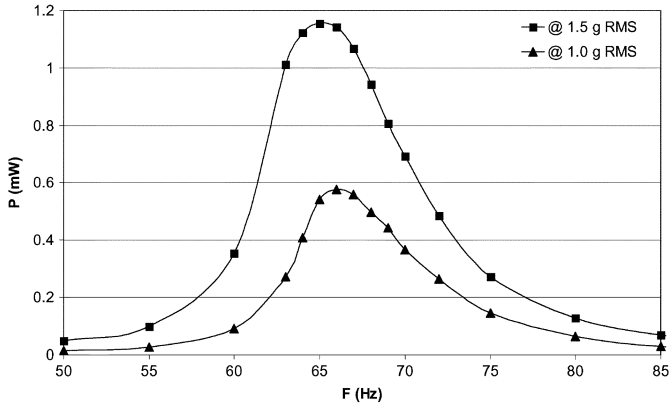

Fig. 9. Load average powers versus vibration frequency for 1.0 and 1.5 g RMS accelerations, with 12 kΩ load resistance.

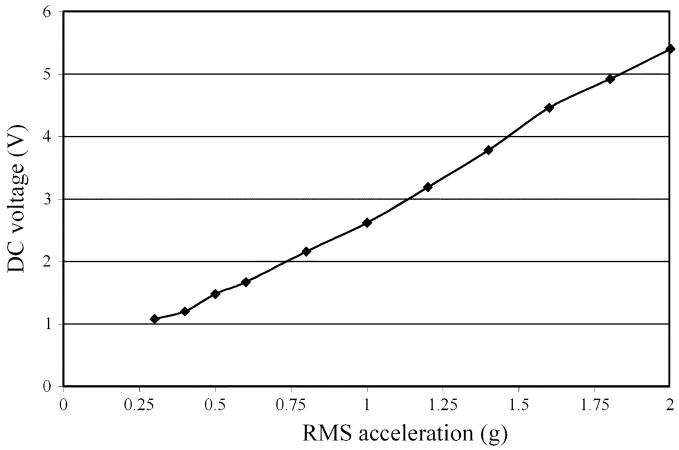

Fig. 10. DC voltage versus mechanical acceleration at resonance frequency with 12 kΩ load resistance.

Then, the final goal has been to optimize the recharging of a 4.8-V NiMH battery, composed of two 2.4-V cells $B1$ and $B2$ in series (see Fig. 11), while minimizing the converter losses and the consumption of the MOSFET control circuit. This control circuit (*IC1*) is in fact based on a low power 32.768 kHz crystal clock (OV-1564-C2, Micro Crystal, Switzerland) with typical supply voltages in the 1.2 to 5.5 V range. The clock current consumption is below 0.5 μA, with a 45% fixed duty cycle.

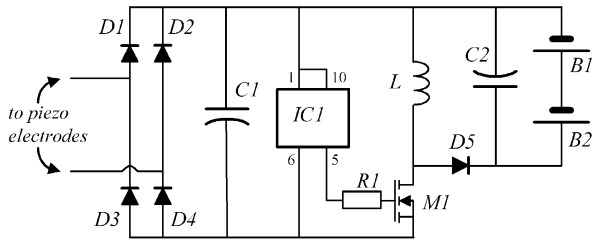

Fig. 11. Experimental circuit diagram.

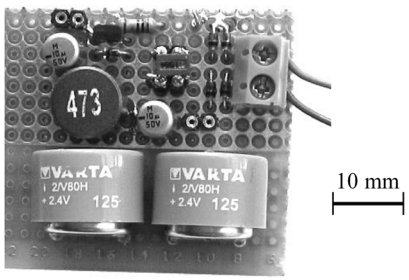

Fig. 12. Buck-boost converter prototype and the 4.8-V NiMH battery.

According to the battery voltage and the clock duty cycle, theoretical maximum value of the input voltage for DCM operation of the buck-boost converter is 5.87 V. The maximum rectified voltage being practically 5.5 V, the crystal duty cycle is appropriate for controlling the transistor. Moreover, the crystal clock was shown to be able to directly drive the transistor gate through a 10 kΩ resistor $(R1)$, starting from supply voltages as low as 1.1 V. A 10-μF capacitor $(C1)$ is connected to the rectifier output. This value is chosen so that the voltage ripple is negligible (i.e., the time constant R_mC1 is much larger than the mechanical vibration half period). A 10-μF additional capacitor $(C2)$ reduces the ripple current across the battery and thus preserves its lifetime. The transistor $(M1)$, a ZVNL110 MOSFET (Zetex), was chosen in particular for its very low threshold gate voltage -0.8 V). All the diodes ($D1$ to $D5$) are BAT86 Schottky diodes. With the above practical parameters, the 47-mH inductor (L) used would theoretically lead to 15.2 kΩ "average input resistance" of the DCM buck-boost converter. A picture of the converter prototype is shown on Fig. 12.

Experimental measurements show that the average input resistance of the converter is not perfectly constant, but maximum and minimum values remain between 11.3 kΩ and 16.4 kΩ (Fig. 13) so that the generator's power is always very close to its maximum. Figs. 14 and 15 show that the powers lost by the rectifier and the buck-boost converter are reasonably weak. The buck-boost converter efficiency is between 84% and 88% for input voltages between 1.6 and 5.5 V. Overall efficiency including the rectifier losses, buck-boost converter losses and control consumption is between 71% and 79% for output power starting from 200 μW up to 1.5 mW.

V. Discussion

Like many sensorless controls based on systems models, the presented "open-loop" power optimization approach is not adaptive with the generator's parameters changes. In practice, parameters changes are mainly due to temperature variations and also

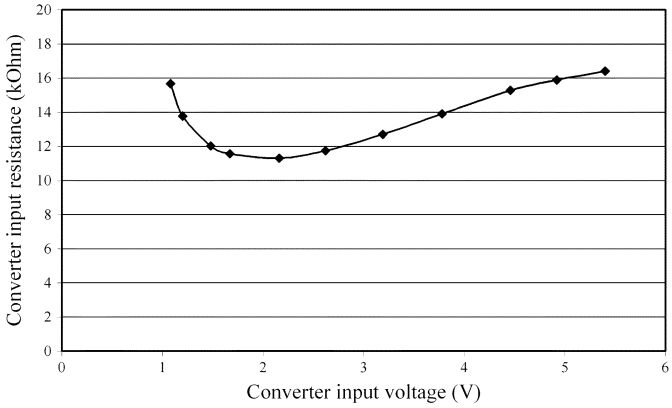

Fig. 13. Converter input average resistance versus input voltage.

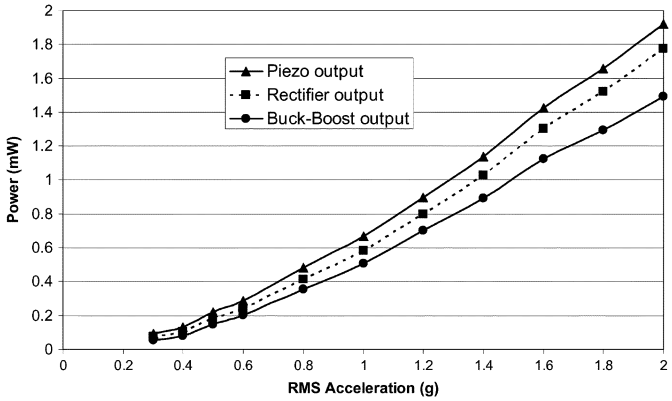

Fig. 14. Average powers versus vibration acceleration at resonance frequency.

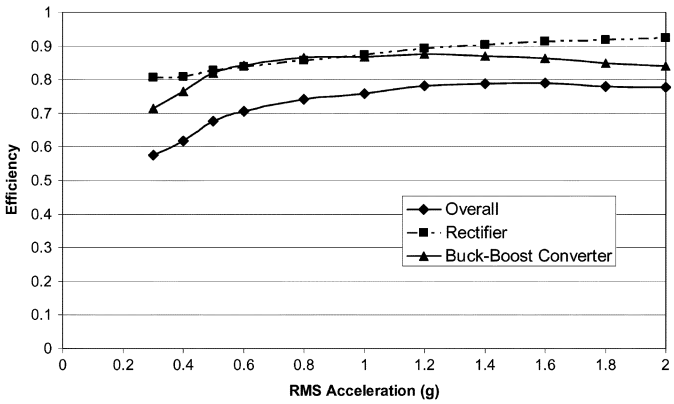

Fig. 15. Efficiencies versus vibration acceleration at resonance frequency.

ageing of the device. However, excepted in case of severe conditions of operation with large temperature variations and/or extreme level of mechanical stress, no more than 10% variations of the matching load resistance can be reasonably expected.

Energy storage is here ensured by a rechargeable battery, but the presented power optimization circuit may also work with a capacitor or a supercapacitor instead of a battery. However, variable output voltage is more constraining than fixed output voltage for ensuring DCM operation of the converter.

Miniaturization of the converter circuit using surface mount technology (SMT) components has been envisioned, but has encountered in particular the problem of important losses for 47-mH SMT inductors. Indeed, such large inductor values inevitably require windings with lots of turns, making the components either bulky or with important losses. The ways to both improving the efficiency and reducing the circuit size would be first to reducing the switching frequency (for instance down to a kilohertz) in order to lowering the switching losses and the control circuit consumption, and then to reducing the duty cycle so that it would be possible to use SMT inductors of a few microhenrys designed for power conversion. A slight improvement of the rectifier efficiency would be also possible using synchronous rectification techniques, as demonstrated by Xu *et al.* [25]. Increasing industrial demand for self-powered devices will otherwise definitely stimulate the development of specific integrated circuits [25] which will enable significant size reductions in the near future.

Miniature electromagnetic generators, also used for energy harvesting, have electromechanical behaviours close to those of piezoelectric generators. Their powers depend on similar ways upon load resistances [28], so optimization of such devices is also possible using the proposed circuit and control.

VI. Conclusion

This paper focuses on power optimization of miniature seismic piezoelectric energy harvesters, which convert surrounding vibrations into electrical energy, and which may be used in particular as power sources for autonomous sensing networks. The power optimization analysis is based on a simple lumped model of the piezoelectric generator and an electrical circuit composed of a full bridge rectifier, voltage smoothing capacitor and resistor. This analysis leads to one or two particular values of the load resistance—related to the device electromechanical parameters—which maximize the power. The study of the relation between the input voltage and input current of a buck-boost converter shows that in discontinuous current mode this circuit intrinsically has the properties defined for power optimization. Moreover, consumption of the control circuit of the buck-boost converter, which requires neither sensors nor sophisticated algorithm, can be easily minimized. These properties are experimentally verified on a 1.5-mW prototype used as a battery charger, showing an effective sensorless tracking of the piezoelectric generator's optimal working points for mechanical accelerations between 0.3 g and 2.0 g RMS. Efficiency of the buck-boost converter, taking into account the control circuit consumption, reaches 88% and remains above 84% for input voltages between 1.6 and 5.5 V. This study and the results presented herein, which can be used as well for optimizing electromagnetic energy harvesters, may be helpful for the design of future integrated interfaces specialized in power optimization of miniature generators.

Appendix
Derivation of the Piezoelectric Generator Output Power

To solve (1)–(3) with the piezoelectric element connected to the rectifier circuit shown on Fig. 2, the relation between the average value of the rectified voltage $V_{\rm rect}$ and the displacement magnitude of $(u_2 - u_1)$ must be first established. For notation simplicity, the relative displacement $(u_2 - u_1)$ is noted

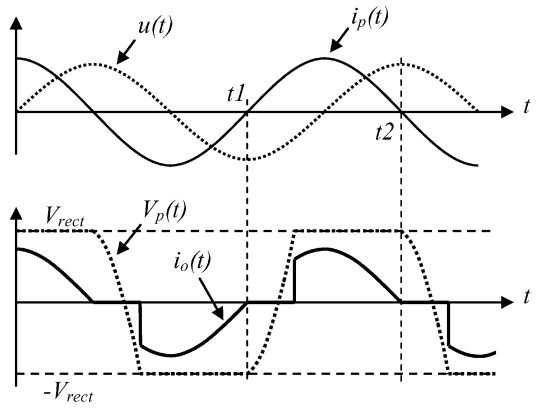

Fig. 16. Typical waveforms of displacement $u(t)$, currents $i_p(t)$ and $i_o(t)$ and voltage $V_p(t)$.

u. The generator's base displacement u_1 is assumed to be sinusoidal with magnitude U_{1M}. The steady-state solution of u is assumed to be sinusoidal too, with magnitude U_M and with same frequency f as $u_1 : u = U_M \sin(\omega t)(\omega = 2\pi f)$. The time constant $\mathrm{RC}_{\mathrm{rect}}$ is assumed to be much larger than the vibration period $T = 1/f$ so that the rectified voltage V_{rect} can be considered as constant end equal to its average value $\langle V_{\mathrm{rect}} \rangle$. Typical waveforms of displacement $u(t)$, currents $i_p\ (t)$ and $i_o(t)$ and voltage $V_p(t)$ are represented on Fig. 16. Let $t1$ and $t2$ be two time instants such that the displacement u goes from a minimum $-U_M$ to a maximum U_M, as illustrated on Fig. 16 $(t1 - t2 = T/2)$. The steady-state average current flowing through C_{rect} is null, and thus

$$\int_{t1}^{t2} i_o dt = \frac{T}{2}\frac{V_{\mathrm{rect}}}{R}. \tag{14}$$

According to (2) and Fig. 2, the current i_o can be expressed as (15). Integration of (15) from time $t1$ to $t2$ and (14) give the relation (16) between the rectified voltage and the relative displacement magnitude

$$i_o = \alpha \frac{du}{dt} - C_p \frac{dV_p}{dt} \tag{15}$$

$$\frac{T}{2}\frac{V_{\mathrm{rect}}}{R} = 2\alpha U_M - 2C_p V_{\mathrm{rect}}. \tag{16}$$

The next step consists in establishing the relationship between the magnitude U_M of relative displacement and the displacement magnitude of the generator's base U_{1M}. Equations (1) and (3) lead to (17) defining the dynamic equilibrium of the system. The term on the right side of this equation is the inertial force F resulting from the base displacement of the generator and driving the electromechanical oscillator. Assume that $u_1 = U_{1M} \sin(\omega t + \varphi)$, the driving force expression is thus $F = M\omega^2 U_{1M} \sin(\omega t + \varphi), \varphi$ being the phase shift with the relative displacement u

$$M\frac{d^2u}{dt^2} + C_v\frac{du}{dt} + (K_S + K_{PE})u + \alpha V_p = -M\frac{d^2u_1}{dt^2}. \tag{17}$$

Let (17) multiplied by du/dt and (15) multiplied by V_p. Integration of these two equations from time $t1$ to $t2$ give the (18) of the energy balance

$$\int_{t1}^{t2} \alpha V_p \frac{du}{dt} dt = \int_{t1}^{t2} V_p i_o dt + \int_{t1}^{t2} C_v \left(\frac{du}{dt}\right)^2 dt \tag{18}$$

with

$$\int_{t1}^{t2} \alpha V_p \frac{du}{dt} dt = \frac{\pi}{2} M\omega^2 U_{1M}^2 U_M \sin(\varphi)$$

$$\int_{t1}^{t2} V_p i_o dt = \frac{\pi}{\omega}\frac{V_{\mathrm{rect}}^2}{R}$$

and

$$\int_{t1}^{t2} C_v \left(\frac{du}{dt}\right)^2 dt = \frac{\pi}{2} C_v \omega U_M^2. \tag{19}$$

At the generator's resonance frequency f_r, the phase shift between the driving force F and the relative displacement u is $\varphi = \pi/2$. For this operating condition, (16), (18) and (19) give the relation (20) between U_{1M} and V_{rect}. The average electrical power P produced by the generator can be expressed as (21). Equations (20) and (21) finally give the expression (4) of the average power P as a function of the electromechanical system parameters, the displacement U_{1M} and the load resistance R at the resonance angular frequency $\omega_r (\omega_r = 2\pi f_r)$

$$M\omega_r^2 U_{1M}^2 U_M = V_{\mathrm{rect}} \left(\frac{2\alpha}{\pi/2 + RC_p\omega_r} + C_v \frac{\pi/2 + RC_p\omega_r}{\alpha R}\right) \tag{20}$$

$$P = \frac{V_{\mathrm{rect}}^2}{R}. \tag{21}$$

REFERENCES

[1] J. Krikke, "Sunrise for energy harvesting products," *IEEE Pervasive Comput.* vol. 4, no. 1, pp. 4–35, Jan./Mar. 2005.

[2] J. A. Paradiso and T. Starner, "Energy scavenging for mobile and wireless electronics," *IEEE Pervasive Computing* vol. 4, no. 1, pp. 18–27, Jan./Mar. 2005.

[3] S. Roundy, E. S. Leland, J. Baker, E. Carleton, E. Reilly;, E. Lai, B. Otis, J. M. Rabaey, P. K. Wright, and V. Sundararajan, "Improving power output for vibration-based energy scavengers," *IEEE Pervasive Comput.* vol. 4, no. 1, pp. 28–36, Jan./Mar. 2005.

[4] N. S. Shenck and J. A. Paradiso, "Energy scavenging with shoe-mounted piezoelectrics," *IEEE Micro*, vol. 21, no. 3, pp. 30–42, May/Jun. 2001.

[5] N. M. White, P. Glynne-Jones, and S. P. Beeby, "A novel thick-film piezoelectric micro-generator," *Smart Mater. Struct.*, vol. 10, pp. 850–852, 2001.

[6] A. Kasyap, J.-S. Lim, D. Johnson, S. Horowitz, T. Nishida, K. Ngo, M. Sheplak, and L. Cattafesta, "Energy reclamation from a vibrating piezoceramic composite beam," in *Proc. 9th Int. Congr. Sound Vibr. (ICSV9)*, Jul. 8–11, 2002.

[7] G. Poulin, E. Sarraute, and F. Costa, "Generation of electric energy for portable devices: Comparative study of an electromagnetic and a piezoelectric system," *Sens. Act. A*, vol. 116, pp. 461–471, 2004.

[8] S. Roundy and P. K. Wright, "A piezoelectric vibration based generator for wireless electronics," *Smart Mater. Struct.*, vol. 13, pp. 1131–1142, 2004.

[9] F. Lu, H. P. Lee, and S. P. Lim, "Modeling and analysis of micro piezoelectric power generators for micro-electromechanical-systems applications," *Smart Mater. Struct.*, vol. 13, pp. 57–63, 2004.
[10] Y. B. Jeon, R. Sood, J. H. Jeong, and S. G. Kim, "MEMS power generator with transverse mode thin film PZT," *Sens. Act. A*, vol. 122, pp. 16–22, 2005.
[11] L. Mateu and F. Moll, "Optimum piezoelectric bending beam structures for energy harvesting using shoe inserts," *J. Intell. Mater. Syst. Struct.*, vol. 16, pp. 835–845, 2005.
[12] K. Mossi, C. Green, Z. Ounaies, and E. Hughes, "Harvesting energy using a thin unimorph prestressed bender: Geometrical effects," *J. Intell. Mater. Syst. Struct.*, vol. 16, pp. 249–261, 2005.
[13] H. S. Yoon, G. Washington, and A. Danak, "Modeling, optimization, and design of efficient initially curved piezoceramic unimorphs for energy harvesting applications," *J. Intell. Mater. Syst. Struct.*, vol. 16, pp. 877–888, 2005.
[14] E. Minazara, D. Vasic, F. Costa, and G. Poulain, "Predictive energy harvesting from mechanical vibration using a circular piezoelectric membrane," in *Proc. IEEE Ultrason. Symp.*, 2005, vol. 2, pp. 946–949.
[15] S. W. Arms, C. P. Townsend, D. L. Churchill, J. H. Galbreath, and S. W. Mundell, "Power management for energy harvesting wireless sensors," in *Proc. SPIE Int. Symp. Smart Struct. Smart Mater.*, San Diego, CA, 2005, vol. 5763, pp. 267–275.
[16] N. Elvin, A. Elvin, and D. H. Choi, "A self-powered damage detection sensor," *J. Strain Anal.*, vol. 38, pp. 115–24, 2003.
[17] T. H. Ng and W. H. Liao, "Sensitivity analysis and energy harvesting for a self-powered piezoelectric sensor," *J. Intell. Mater. Syst. Struct.*, vol. 16, pp. 785–97, 2005.
[18] G. K. Ottman, A. C. Bhatt, H. Hofmann, and G. A. Lesieutre, "Adaptive piezoelectric energy harvesting circuit for wireless remote power supply," *IEEE Trans. Power Electron.*, vol. 17, pp. 669–676, Sep. 2002.
[19] G. K. Ottman, H. Hofmann, and G. A. Lesieutre, "Optimized piezoelectric energy harvesting circuit using step-down converter in discontinuous conduction mode," in *Proc. IEEE Power Electron. Spec. Conf.*, Jun. 23–27, 2002, vol. 4, pp. 1988–1994.
[20] G. K. Ottman, H. Hofmann, and G. A. Lesieutre, "Optimized piezoelectric energy harvesting circuit using step-down converter in discontinuous conduction mode," *IEEE Trans. Power Electron.*, vol. 18, no. 2, pp. 696–703, Mar. 2003.
[21] J. Han, A. Von-Jouanne, T. Le, K. Mayaram, and T. S. Fiez, "Novel power conditioning circuits for piezoelectric micro power generators," in *Proc. IEEE Appl. Power Electron. Conf. Expo. (APEC)*, 2004, vol. III, pp. 1541–1546.
[22] E. Lefeuvre, A. Badel, C. Richard, and D. Guyomar, "High-performance piezoelectric vibration energy reclamation," in *Proc. SPIE Int. Symp. Smart Struct. Smart Mater.*, San Diego, CA, Mar. 14–18, 2004, vol. 5390, pp. 379–387.
[23] S. Ben-Yaakov and N. Krihely, "New resonant rectifier for capacitive sources," in *Proc. 23rd IEEE Conv. Electr. Electron. Eng.*, Sep. 6-7, 2004, pp. 48–51.
[24] E. Lefeuvre, A. Badel, C. Richard, and D. Guyomar, "Piezoelectric energy harvesting device optimization by synchronous electric charge extraction," *J. Intell. Mater. Syst. Struct.*, vol. 16, pp. 865–876, Oct. 2005.
[25] S. Xu, K. D. T. Ngo, T. Nishida, G.-B. Chung, and A. Sharma, "Converter and controller for micro-power energy harvesting," in *Proc. 20th Annu. Appl. Power Electron. Conf. Expo*, Austin, TX, 2005, vol. 1, pp. 226–230.
[26] E. Lefeuvre, A. Badel, C. Richard, L. Petit, and D. Guyomar, "A comparison between several vibration-powered piezoelectric generators for standalone systems," *Sens. Actuators A*, vol. 126, pp. 405–416, 2006.
[27] H.-W. Joo, C.-H. Lee, J.-S. Rho, and H.-K. Jung, "Identification of material constants for piezoelectric transformers by three-dimensional, finite-element method and a design-sensitivity method," *IEEE Trans. Ultrason. Ferroelectr. Freq. Contr.*, vol. 50, no. 8, pp. 965–971, Aug. 2003.
[28] P. Glynne-Jones, M. J. Tudor, S. P. Beeby, and N. M. White, "An electromagnetic, vibration-powered generator for intelligent sensor systems," *Sens. Actuators A*, vol. 110, pp. 344–349, 2004.

Elie Lefeuvre was born in France in 1971. He received the B.S. degree in electrical engineering from Paris-XI University, Paris, France, in 1994, the M.S. degree from the Institut National Polytechnique de Toulouse, Toulouse, France, in 1996, and the Ph.D. degree from Laval University of Québec, Québec City, QC, Canada, in 2001.

In 2002, he became an Assistant Professor at the Institut National des Sciences Appliquées (INSA) de Lyon, Lyon, France, where he joined the Laboratoire de Génie Electrique et Ferroélectricité. His current research activities include piezoelectric systems, energy harvesting, vibration control, and noise reduction.

David Audigier was born in France in 1966. He received the B.S. degree from Lyon I University, Lyon, France, in 1988, and the M.S. and Ph.D. degrees from the Institut National des Sciences Appliquées de Lyon (INSA de Lyon), Lyon, France, in 1990 and 1996, respectively, all in electrical engineering.

In 1997, he became an Assistant Professor at the INSA de Lyon, where he joined the Laboratoire de Génie Electrique et Ferroélectricité. His current research activities include piezoelectric systems, energy harvesting, vibration control and noise reduction, and characterization and power applications of piezoelectric materials.

Claude Richard was born in 1965. He received the M.S. degree in electrical engineering and the Ph.D. degree in acoustics from the Institut National des Sciences Appliquées de Lyon (INSA de Lyon), Lyon, France, in 1988 and 1992, respectively.

After a postdoctoral study on 1.3 piezocomposite materials at the Underwater Sound Reference Detachment, Naval Research Laboratory (NRL/USRD), Orlando, FL, in 1993, he got a position at INSA de Lyon where he has since worked on the applications of piezoelectric ceramics since 1994. He is currently a Professor of electrical engineering at INSA de Lyon where he manages the Electroactive Systems Team, Laboratoire de Génie Electrique et Ferroélectricité. His research interests include, nonlinear switched piezo devices for vibration damping and energy harvesting, 1-3 piezocomposites (dice and fill and piezo fiber composite types), power applications of piezoelectrics, and material characterization.

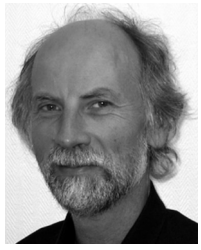

Daniel Guyomar received the B.S. degree in physics from Amiens University, Amiens, France, the M.S. and Doc.Eng. degrees in acoustics from Compieègne University, Compiègne, France, and the Ph.D. degree in physics from Paris VII University, Paris, France.

From 1982 to 1983, he was a Research Associate in fluid dynamics at the University of Southern California, Los Angeles. He was a National Research Council Awardee (1983–1984) detached at the Monterey Naval Postgraduate School, California, to develop transient wave propagation modelling. He was hired in 1984 by Schlumberger to lead several projects dealing with borehole imaging, then he moved to Thomson Submarine activities in 1987 to manage the research activities in the field of underwater acoustics. In 1992, he co-created the Techsonic company, which is involved in research, development, and production of piezoelectric and ultrasonic devices. He is presently a full-time University Professor at the Institut National des Sciences Appliquées de Lyon (INSA), Lyon, France, where he manages the Laboratoire de Génie Electrique et Ferroélectricité and is consultant for several companies. His present research interests are in the field of piezo-material characterization, piezo-actuators, acoustics, power ultrasonics, vibration control, and energy harvesting.